Journal of the Korean Society for Nondestructive Testing
Vol. 27, No. 6 (2007. 12)

Health Monitoring of a Composite Actuator with a PZT Ceramic during Electromechanical Fatigue Loading

Sung Choong Woo*,† and Nam Seo Goo**

Abstract This work describes an investigation into the feasibility of using an acoustic emission (AE) technique to evaluate the integrity of a composite actuator with a PZT ceramic under electromechanical cyclic loading. AE characteristics have been analyzed in terms of the behavior of the AE count rate and signal waveform in association with the performance degradation of the composite actuator during the cyclic tests. The results showed that the fatigue cracking of the composite actuator with a PZT ceramic occurred only in the PZT ceramic layer, and that the performance degradation caused by the fatigue damage varied immensely depending on the existence of a protecting composite bottom layer. We confirmed the correlations between the fatigue damage mechanisms and AE signal types for the actuators that exhibited multiple modes of fatigue damage; transgranular micro damage, intergranular fatigue cracking, and breakdown by a short circuiting were related to a burst type signal showing a shortly rising and slowly decaying waveform with a comparably low voltage, a continuous type signal showing a gradual rising and slowly decaying waveform with a very high voltage and a burst and continuous type signal with a high voltage, respectively. Results from the present work showed that the evolution of fatigue damage in the composite actuator with a PZT ceramic can be nondestructively identified via in situ AE monitoring and microscopic observations.

Keywords: Electromechanical Fatigue, Composite Actuator with a PZT Ceramic, Acoustic Emission, Degradation

1. Introduction

Due to their outstanding displacement performance and high load capability, piezoelectric actuators (Chung et al., 2006; Mossi et al., 2006; Schwartz et al., 2002; Zhang et al., 1999) are widely used in the tail wing of micro air-vehicles, micro-pumps for drug delivery systems and synthetic jet actuators, as well as in other fields of biomimetic fish robots. The performance of piezoelectric composite actuators, in particular, can be manipulated and maximized by controlling the stacking sequence during their hand layup procedures or by controlling drive frequencies and applied electric fields during the actuation process. However, the constituent PZT ceramic is susceptible to fracturing or cracking on account of the inborn high brittleness. The nucleation of fatigue damages in piezoelectric composite actuators results in a significant reduction in performance, ultimately leading to failure. Piezoelectric actuators are usually subjected to a prolonged out-of-plane cyclic condition. Thus, an experimental investigation of the initiation and evolution of fatigue damages is necessary for gaining a better understanding of the safety and integrity of piezoelectric actuators.

Even though failures in engineering

Received: October 29, 2007, Accepted: December 18, 2007. * Artificial Muscle Research Center, Konkuk University, 1 Hwayang-dong, Gwangjin-gu, Seoul 143-701, ** Smart Microsystem Research Laboratory, Department of Advanced Technology Fusion, Artificial Muscle Research Center and Smart Robot Center, Konkuk University, 1 Hwayang-dong, Gwangjinu, Seoul 143-701, † Corresponding author: lilsuzy@hanyang.ac.kr

applications usually occur via cyclic loading, there is very little consistency in the useful information/data for the design of the piezoelectric composite actuator. A considerably small amount of research has been done in the field of the structural integrity of smart structures and materials. One key field in the structural integrity of smart structures/materials is their responses under a fatigue loading environment. Until now, virtually most researches related to fatigue of smart structure have been either focused on mechanical fatigue (White et al., 1994) of the structure or electric fatigue (Mizuno et al., 2005; Liu et al., 2005; Zhang et al., 2004) studies of piezoelectric material itself on the performance characteristics of piezoelectric actuators.

In previous studies, we addressed composite actuators with a thin sandwiched PZT plate using a woven fabric type composite system and investigated how the thickness of embedded PZT ceramic and the lay-up sequence affected their flexural displacement performances via a three-dimensional finite element simulation (Woo et al., 2007a). We have also elucidated the influences of dome height and stored elastic energy on the actuating performance of a plate-type piezoelectric composite actuator experimentally (Woo et al., 2007b). Mechanical bending fracture process for piezoelectric composite actuators has been discussed by analyzing dominant frequency bands and the classification of waveform patterns with the aid of acoustic emission (AE) monitoring (Woo et al., 2006; Woo et al., 2007c–d).

We now present an AE-based nondestructive evaluation technique (Eitzen et al. 1984) to obtain information on the initiation and propagation of electromechanically induced fatigue damage in composite actuators with a PZT ceramic. After the fatigue tests, we identified the fatigue failure mechanisms by analyzing the characteristics of the AE count rate and signal waveforms.

2. Experimental

2.1 Preparation of Specimens

As illustrated in Fig. 1, two different layup sequences were used to fabricate the actuating specimens. Specimen-1 consists of four layers without a bottom layer, whereas specimen-2 consists of five layers with a glass-epoxy bottom layer that protects the PZT ceramic. Specimen-1 without the glass-epoxy bottom layer was included for a test object in order to investigate how the protecting bottom layer affects the fatigue damages and the actuating performance. The common feature of these actuators is that they are stacked such that the PZT ceramic is placed apart from the actuator's neutral plane, and thus they have good displacement performances. The specimens were manufactured with woven fabric carbon-epoxy prepregs (WSN1K-B), woven fabric glass-epoxy prepregs (GEP108), and a PZT ceramic (3203HD). Details of the material properties can be found in (Woo et al., 2007b). Specimens which were laminated in a hand layup procedure were co-cured at a temperature of 177 ℃ in an autoclave in accordance with the curing cycle for three hours.

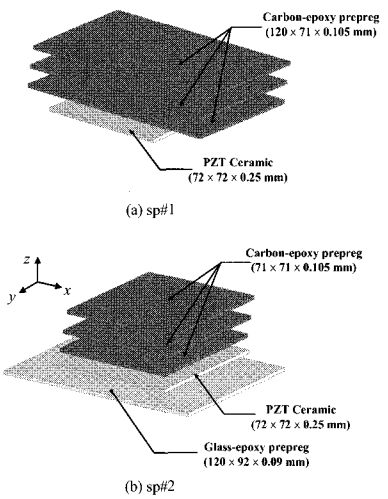

Fig. 1 Schematic of two kinds of actuating specimens used in electromechanical cyclic tests

2.2 Electromechanical Cyclic Tests

Fig. 2 shows the actuating mechanism of a composite actuator with a PZT ceramic. Piezoelectric composite actuators used in the study are composed of fiber composite and PZT ceramic layers. The poling direction of the PZT is along the z-axis, from the bottom to the top. When the actuator is stacked such that the PZT ceramic is placed apart from the actuator's neutral plane, the PZT layer deforms in an in-plane direction when subjected to an electric field. As such, an asymmetrically laminated plate with PZT ceramic displays bending deformation. If a negative voltage is applied to the PZT ceramic, it contracts in an in-plane direction and the composite actuator thereupon bends upward, as illustrated in Fig. 1. Conversely, when positive voltage is applied, the PZT expands in the same direction, and the actuator is consequently flattened.

As illustrated in Fig. 3, we placed the specimens on two supporting jigs separated by a distance of 72 mm. We then performed fatigue tests until 10^7 cycles by providing an electric field for the PZT ceramic via a high-voltage signal function generator (TD-2 Power Supplier), which was connected to a digitizing oscilloscope (HP 54622A). Next we applied a mechanical loading to the upper surface of the specimen by using a weight of 2 N. The specimens were excited at their resonance frequencies with an AC input voltage equivalent to a peak-to-peak voltage of 300 V_{pp} in the form of a sinusoidal wave. It is widely recognized that piezoelectric actuators produce a maximum displacement performance at the resonant frequency. The resonance frequencies were determined experimentally to be 24 Hz for specimen-1 and 13 Hz for specimen-2. The mean values of the electric fields were set at zero; thus, an amplitude ratio of $R = E_{min}/E_{max} = -1$ prevails. The bending actuating displacement was measured at the center portion of the specimens by using a noncontact-type laser displacement system (Keyence LK-081). We tested three specimens for each actuator type, and the result presented here is a typical one.

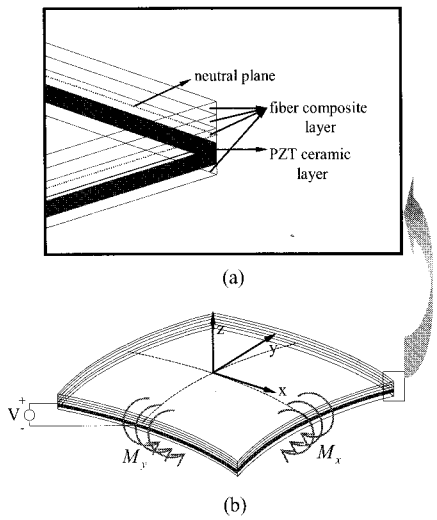

Fig. 2 Actuating mechanism of a composite actuator with a PZT ceramic: (a) before applying an electric field. (b) after applying an electric field

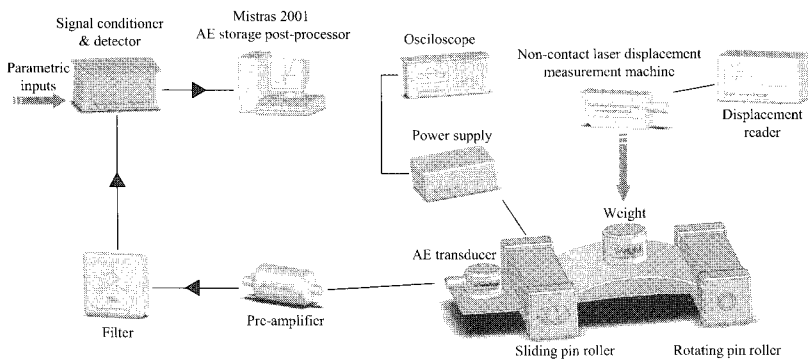

Fig. 3 Experimental arrangement for electromechanical cyclic tests with AE monitoring

2.3 In Situ AE Monitoring and Fractography

In situ monitoring of fatigue damages within the specimens was accomplished with the aid of the AE signal acquisition and processing package MISTRAS 2001 of Physical Acoustics Corporation. An AE sensor was attached to one side tab of the test specimen by means of a coupling agent. The AE sensor having a 265 kHz central frequency connected to a data acquisition board that was incorporated into a personal computer. Pre-amplification of 40 dB and band-pass filtering of 10 kHz to 1200 kHz were performed by a pre-amplifier. For the AE acquisition parameters, we used a threshold level of 45 dB considering the vibration noise of the specimens during actuating, a sampling rate of 4 MHz, and a hit lockout time of 1 ms. Pencil lead break tests were performed for the calibration of the applied setup. We then monitored the AE signals in real time as the actuating displacement was recorded. The monitoring continued until the number of cycles reached 10^7 or until the specimen finally failed. After testing, mechanical and electrical noises detected with signals having duration less than 25 μs were all screened (Woo et al., 2007) in the AE parametric analysis. The specimen was carefully disassembled to avoid any damage and then the damage zone induced by electric cyclic fatigue was examined by using a scanning electron microscopy (SEM) and a reflected optical microscopy.

3. Results and Discussion

3.1 Fractographic Analysis Results

Fig. 4 shows the SEM observations of specimen-1. Fig. 4(a) is the surface of a PZT ceramic before fatigue testing and thus shows undamaged grains and their boundaries with an average diameter of 1~3 μm. In Fig. 4(b), we can observe the fatigued surface loaded up to 1.6 x 10^6 cycles where the transgranular micro-damage is dominant but the damages at the grain boundary are hardly seen. In Fig. 4(c), on the other hand, it is observed that conspicuous intergranular fatigue cracking propagated along the grain boundaries across the center of the

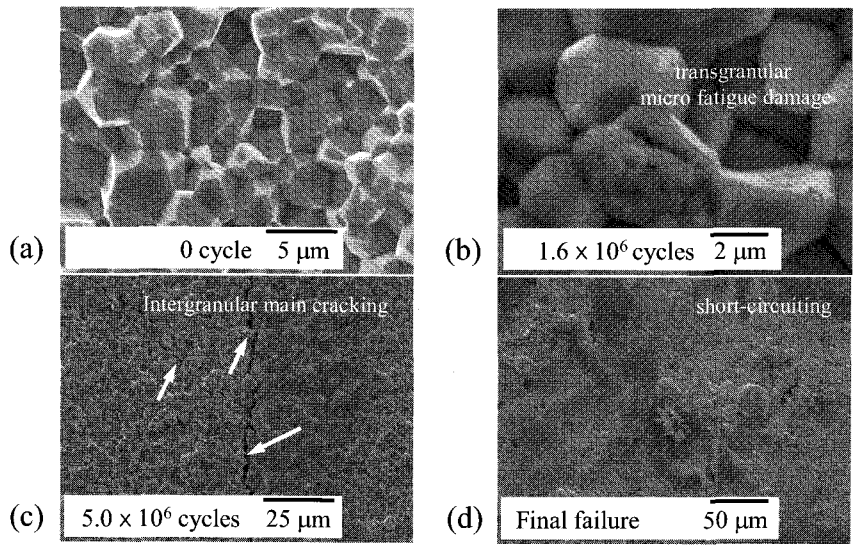

Fig. 4 SEM images for specimen 1: (a) the unfatigued surface of PZT ceramic (b) micro-damage in the grain of a PZT layer, (c) fatigue cracking and (d) pores and dimples caused by short-circuiting

surface. This main fatigue cracking was occurred nearly at the end of the loading cycles and it was visible to the naked eye. We can also see that the surface of the PZT ceramic was melted down by a high electric field on either side of the fatigue cracking, though, aside from the cracking, the transgranular fatigue damage is still extensive in other areas. Fig. 4(d) shows many pits, pores and dimples induced by a short-circuiting in the PZT ceramic layer during the final failure.

Reflected-light microscopy was used on the polished surface of specimen-1 to examine the internal damage state in fiber composites and PZT ceramic layers in the through-width direction. One portion, area A as shown in Fig. 5, was cut carefully from specimen-1 by using a diamond wheel saw and then the cutting surface was ground and polished using 0.05 μm alumina powder to achieve sufficiently low surface roughness. Fig. 5 shows the polished micrograph of specimen-1. From the Fig. 5, it is confirmed that the crack originated from the surface of PZT ceramic layer propagated into the carbon fiber composite layer. However, there is no damage such as delamination between PZT ceramic and carbon fiber composite layers. That is to say, the fatigue crack formed in the PZT ceramic layer did not develop in to the fiber composite layer. Such fatigue crack in the PZT ceramic layer must have considerably affected the displacement performance and the fatigue life of specimen-1, which will be discussed in the following section.

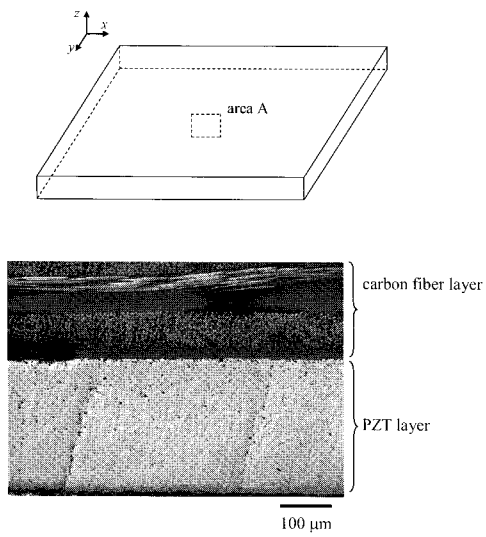

Fig. 5 Cross-sectional micrograph showing the each layer of specimen-1

Fig. 6 is a reflected optical microscopy showing the microstructure in each layer of specimen-2. In contrast to specimen-1, fatigue damages are not observed as shown in Fig. 6, suggesting that surface fatigue crack in the PZT ceramic layer did not occur or it, if occurred, could not propagated into the internal part of the PZT ceramic because the glass fiber bottom layer protected the PZT ceramic.

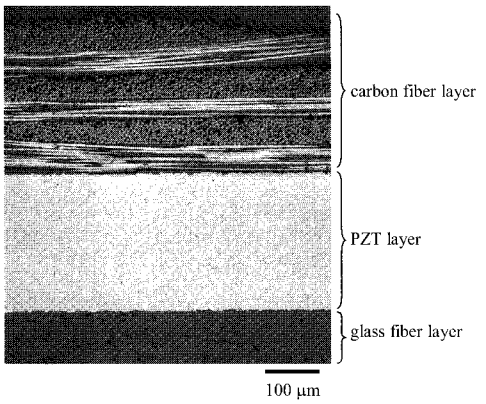

Fig. 6 Cross-sectional micrograph showing the each layer of specimen-2

3.2 Performance Degradation and AE Characteristics

Fig. 7 shows a typical displacement–cycle curve as well as the behavior of the AE count rate for specimen-1. The AE count rate in Fig. 7 is defined as the number of AE event hits every 10^5 cycles. In the case of specimen-1, the initial actuating displacement was 4.58 mm. There is no displacement reduction and any AE signals while the number of cycles reaches 2.6×10^5 where the first AE event begins to appear. However, a high AE count rate occurred together with a 20 % reduction in actuating displacement at about 3.0×10^5 cycles, suggesting that fatigue crack began

to occur and rapidly grew only in the PZT ceramic layer. This is reasonable considering that PZT ceramic is a very brittle material. Subsequently, the actuating displacement degradation continued at a much slower rate until 4.3×10^6 cycles and the AE count rate was low level. After that, the actuating displacement decreased again immensely along with a maximum count rate at 4.3×10^6 cycles. Considering the high AE count rate and the large reduction in actuating displacement, the main cracking in specimen-1 might have initiated and propagated rapidly at this point as observed in Fig 4(c). In a range of 4.3×10^6 – 5.2×10^6 cycles, a relatively intermediate AE count rate was detected. Specimen-1 reached the final failure at 5.2×10^5 cycles because of a short-circuiting caused by fatigue cracking in the PZT ceramic layer, which was visible to the naked eye. At the final failure of specimen-1, the actuating displacement was 1.84 mm, which was approximately 60 % less than the initial actuating displacement of 4.58 mm. Hence, the use of specimen-1 without the bottom protecting layer yields a significantly lower actuating displacement under electromechanical cyclic loading.

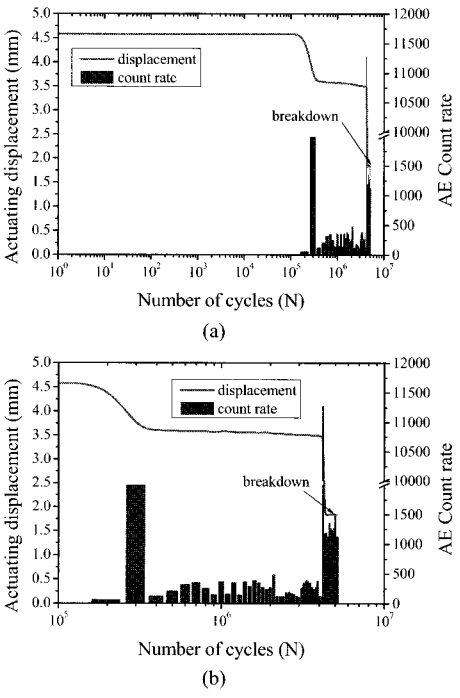

Fig. 7 Actuating displacement versus the AE count rate with an increasing number of cycles for specimen 1: (a) the entire cycling loading range and (b) the loading range between 10^5 and 10^7 cycles.

In the case of specimen-2, as shown in Fig. 8, the actuating displacement is almost constant before 1.5×10^6 cycles and there were no detectable AE events, suggesting that no fatigue damage has yet occurred in specimen-1. The AE signal became detectable at 1.5×10^6 cycles, where a high AE count rate was observed, which indicates that some damages has begin to occur within specimen-2. In the case of specimen-2, the cycle of the damage onset is even later than specimen-1. This result is reasonable considering that a maximum bending stress by the same electric field occurs in the surface of the brittle PZT ceramic layer for specimen-1 while the maximum bending stress takes place in the surface of flexible glass fiber bottom layer for specimen-2. However, it is believed that the damage was not significant because noticeable damages were not observed in both the PZT ceramic and the fiber composite layers as already confirmed in Fig. 6. Therefore, the AE signals generated in the early stage are attributed to the ones such as the transgranular fatigue damages as shown in Fig. 4(c). At this time, the actuating displacement dropped by 8.14 % below the initial actuating displacement of 3.32 mm. As the number of cycles increased to 7.4×10^6 cycles, the drop in displacement was not large and the activity in the AE count rate was not conspicuous but showed only a slight variation. Hence, the initiation and evolution of fatigue damage is not active in the case of specimen-2 during the cycles. From 7.4×10^6 cycles to 10^7 cycles, the AE count rate is occasionally high and there is also reduction in displacement. Even with the passing of 10^7 cycles, specimen-2 is well actuated without a significant reduction in the

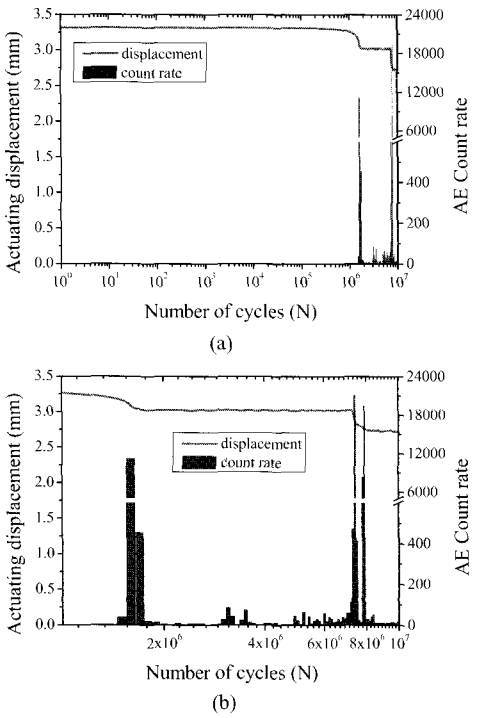

Fig. 8 Actuating displacement versus the AE count rate with an increasing number of cycles for specimen 2: (a) the entire cycling loading range and (b) the loading range between 10^6 and 10^7 cycles.

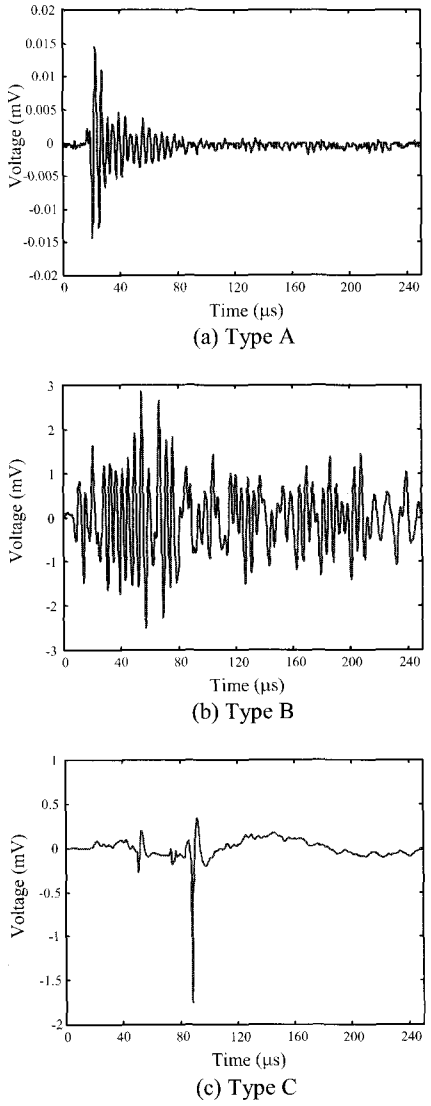

Fig. 9 *Typical waveforms corresponding to the* fatigue failure modes: (a) transgranular micro damage, (b) intergranular fatigue crack propagation and (c) breakdown by a short circuiting

actuating displacement and without any failure. At 10^7 cycles, the measured value of the actuating displacement was 2.73 mm, which is approximately 17.8 % less than the value of the initial actuating displacement of 3.32 mm. It thus appears that the protecting bottom layer retards the growth of fatigue damage or stops cracks from propagating in the PZT ceramic layer.

3.3 Signal Classification

For further investigation on the fatigue damage evolution, we classified the AE signals from the specimens into three types on the basis of the waveform and signal voltage, and the typical waveforms are plotted in Fig. 9. As shown in Fig. 9(a), type A, which was detected during the entire cyclic test, is a burst-type signal showing a shortly rising and slowly decaying waveform with a comparably low voltage. In contrast, type B which was detected only after 4.2×10^6 cycles, exhibits a continuous-type signal with a very high voltage. We suggest, therefore, that a waveform such as type A is formed due to the weak emissions that originate from the transgranular micro-damage in

the PZT ceramic layer, as displayed in Fig. 4(b), and that type B is possibly formed due to the intergranular cracking along the grain boundary during the fatigue crack propagation, as shown in Fig. 4(c). Type C, on the other hand, which was detected only at the breakdown of specimen-1 due to a short-circuiting, shows a burst and continuous type signal with a high voltage. Note also that specimen-2 emitted few type B signals and no type C signals. Hence, as stated already, the lack of intergranular cracking and short-circuiting in specimen-2 may be due to the way the glass-epoxy bottom layer restrains the fatigue damage evolution and/or crack propagation.

4. Conclusions

By analyzing the behavior of the AE event rate and the signal waveform, we were able to elucidate the fatigue damage mechanism of a composite actuator with a PZT ceramic under electromechanical cyclic loading. The initial fatigue damage of the composite actuator with a PZT ceramic was caused by the transgranular damage in the PZT ceramic layer; the final failure was caused by the main crack propagation induced by a short-circuiting along with intergranular cracking, which were directly associated with the performance of the actuators presented here. As the number of cycles increased, a noticeable reduction in displacement coincided with a high AE count rate. The transgranular damage is related to a burst-type signal with a low voltage. Continuous-type signals with an intermediate voltage were due to intergranular cracking. The short-circuiting showed the characteristics of a burst-type signal and a continuous type-signal with a high voltage. Our results confirm that the AE technique is applicable to the health monitoring of a composite actuator with a PZT ceramic, particularly when the actuator is subjected to fatigue caused by a combination of external cycling mechanical loading and internal electrical actuation.

Acknowledgment

The present work was supported by the Korea Research Foundation Grant (KRF-2006-005-J03302). The authors appreciate this financial support.

References

Chung, S. W., Hwang, I. S. and Kim, S. J. (2006) Large-Scale Actuating Performance Analysis of a Composite Curved Piezoelectric Actuator, Smart Materials and Structures, Vol. 15, pp. 213–220

Eitzen, D. G. and Wadley, H. N. G. (1984) Acoustic Emission: Establishing the Fundamentals, Journal of Research of the National Bureau of Standards, Vol. 89, pp. 75–100

Liu, T., Oates, W. S., Wan, S. and Lynch, C. S. (2005) Crack Initiation at Electrode Edges in PZN–4.5%PT Single Crystals, Journal of Intelligent Material Systems and Structures, Vol. 16, pp. 373–379

Mizuno, M. and Honda, Y. (2005) Simplified Analysis of Steady-State Crack Growth of Piezoelectric Ceramics Based on the Continuum Damage Mechanics, Acta Mechanica, Vol. 179, pp. 157–168

Mossi, K., Mouhli, M., Smith, B. F., Mane, P. P. and Bryant, R. G. (2006) Shape Modeling and Validation of Stress-Biased Piezoelectric Actuators, Smart Materials and Structures, Vol. 15, pp. 1785–1793

Schwartz, R. E. and Narayanan, M. (2002) Development of High Performance Stress-Biased Actuators through the Incorporation of

Mechanical Pre-Loads, Sensors and Actuators A, Vol. 101, pp. 322–331

White, G. S., Raynes, A. S., Vaudin, M. D. and Freiman, S. W. (1994) Fracture Behavior of Cyclically Loaded PZT, Journal of the American Ceramic Society, Vol. 77, pp. 2603–2608

Woo, S. C. and Goo, N. S. (2006) Analysis of the Fracture Behavior of Plate-type Piezoelectric Composite Actuators by Acoustic Emission Monitoring, Journal of the Korean Society for Nondestructive testing, Vol. 26, pp. 220–230

Woo, S. C. and Choi, N. S. (2007) Analysis of Fracture Process in Single-Edge-Notched Laminated Composites Based on the High Amplitude Acoustic Emission Events, Composites Science and Technology, Vol. 67, pp. 1451-1458

Woo, S. C. and Goo, N. S. (2007a) Prediction of Actuating Displacement in a Piezoelectric Composite Actuator with a Thin Sandwiched PZT Plate by a Finite Element Simulation, Journal of Mechanical Science and Technology, Vol. 21, pp. 455–464

Woo, S. C. and Goo, N. S. (2007b) Influences of Dome Height and Stored Elastic Energy on the Actuating Performance of a Plate-Type Piezoelectric Composite Actuator, Sensors and Actuators A, Vol. 137, pp. 110–119

Woo, S. C. and Goo, N. S. (2007c) Analysis of the Bending Fracture Process for Piezoelectric Composite Actuators Using Dominant Frequency Bands by Acoustic Emission, Composites Science and Technology, Vol. 67, pp. 1499–1508

Woo, S. C. and Goo, N. S. (2007d) Identification of Failure Mechanisms in a Smart Composite Actuator with a Thin Sandwiched PZT Plate Based on Waveform and Primary Frequency Analyses, Smart Materials and Structures, Vol. 16, pp. 1460–1470

Zhang, X. D. and Sun, C. T. (1999) Analysis of a Sandwich plate Containing a Piezoelectric Core, Smart Materials and Structures, Vol. 8, pp. 31–40

Zhang, X. P., Galea, S., Ye, L. and Mai, Y. W. (2004) Characterization of the Effects of Applied Electric Fields on Fracture Toughness and Cyclic Electric Field Induced Fatigue Crack Growth for Piezoceramic PIC 151, Smart Materials and Structures, Vol. 13, pp. N9–N16